cigre Turkey

TEPES
TURKISH JOURNAL OF ELECTRICAL POWER AND ENERGY SYSTEMS

TEPES, Vol. 4, Issue. 1, 40-49, 2024 **DOI:** 10.5152/tepes.2024.24001

RESEARCH ARTICLE

High Impedance Fault Detection in Medium Voltage Distribution Systems Using Wavelet Transform

Baraa Makkawi, Ömer Usta

Department of Electrical Engineering, İstanbul Technical University, İstanbul, Turkey

Cite this article as: B. Makkawi and Ö. Usta, "High impedance fault detection in medium voltage distribution systems using wavelet transform," *Turk J Electr Power Energy Syst.*, 2024; 4(1), 40-49.

ABSTRACT

Conventional protection systems in distribution systems are capable of identifying low-impedance faults since such faults produce high fault current levels. But in a high impedance fault case protection schemes fail to detect a fault due to the fact that such faults do not generate enough fault current to operate conventional protection devices and fuses. This paper presents a novel algorithm for high impedance fault detection in medium voltage distribution systems. The proposed algorithm leverages multi-resolution analysis using discrete wavelet transform analysis for improved reliability and accuracy, extracting d5 coefficients at the transformer secondary terminal of all phases and the neutral, calculating their energies and integrating and calculating the average slope and comparing them to a threshold slope value in order to take the right decision for high impedance fault detection. The research explores the algorithm's effectiveness through extensive testing using MATLAB/Simulink software, demonstrating its potential as a valuable tool for enhancing the reliability of medium voltage distribution systems.

Index Terms—Discrete wavelet transform, distribution systems, high impedance fault, fault detection, HIF modeling

I. INTRODUCTION

Faults in distribution systems fall under two main categories: low impedance faults and high impedance faults (HIFs). Low impedance faults are very common and can be easily detected with conventional protection devices such as an overcurrent relay and a circuit breaker, on the other hand, HIFs are not easily detected and conventional protection devices fail in detecting and eliminating them.

A HIF is a fault that has a high impedance value, by which the fault current is in the range of normal current in the system and under the maximum load current. So conventional protection devices are not able to detect it. High impedance fault occurs as a result of a contact between an energized conductor and material of high impedance profile such as a tree branch, concrete, gravel, asphalt, sand, cement, and thin gravel. HIFs are influenced by factors such as the ground surface material, surface humidity, weather conditions, load type, feeder configuration, and voltage levels [1]. The factors that have the most influence on HIF are surface humidity and material; higher humidity results in a higher fault current magnitude, and different materials result in different voltage-current characteristics [2, 3].

High impedance faults can cause significant risks, such as the potential for arcing that may lead to fires, especially when the fault occurs in dry vegetation, damaged cable insulation, or insulators. Detecting HIFs requires advanced methods, such as signal processing and machine learning (ML), to recognize the subtle and intermittent characteristics associated with these faults and ensure the safety and reliability of the electrical grid.

A. High Impedance Fault Effect

HIFs have consequences not only on the power system but also on living beings. HIFs are usually accompanied by an arc. During an HIF, flammable gas may be generated, or the evolution of an arc near flammable material may result in fire and explosion [4]. Moreover, due to the generation of current, unintentional contact between the energized conductor and a line crewman or a member of the public or any living being would occur, resulting in fatal conditions [5].

Corresponding author: Baraa Makkawi, makkawi21@itu.edu.tr

Received: January 5, 2024
Revision Requested: January 10, 2024
Last Revision Received: January 22, 2024
Accepted: January 24, 2024
Publication Date: February 20, 2024

HIFs can have several significant effects on power distribution systems, which directly impact the reliability, safety, and operational efficiency of the electrical network and public safety. Key effects that are associated with HIFs are:

- Equipment damage: The arcing associated with HIFs can cause damage to equipment, including transformers, insulators, and other components in the affected portion of the power distribution system.
- Fire hazard: When an HIF occurs in areas with dry vegetation or compromised insulation, arcing occurs, posing a significant fire hazard, leading to potential damage to equipment and posing risks to personnel and nearby structures.
- Danger to the public safety: due to the fact that an HIF generates current and a person or an animal may come into contact with the faulty conductor, this would result in death from electrical shock.

B. High Impedance Fault Characteristics

High impedance faults show some peculiar features that distinguish them from other types of electrical faults. Understanding these features is crucial to the development of effective detection and mitigation strategies.

Here are some key characteristics of HIFs:

- Low fault current levels: Unlike low impedance faults, where a direct and low-resistance path to ground results in high current flows, HIFs involve partial or intermittent connections, leading to lower current levels.
- Voltage fluctuations: HIFs can cause fluctuations in voltage levels within the power distribution system. These fluctuations may be subtle but can affect the stability and reliability of the electrical network.
- Non-linearity: the V-I characteristic curve is usually nonlinear in nature due to the existence of an arc [6, 7].
- Low frequency and high frequency components in voltage and current waveforms: because of the non-linearity of HIF, waveforms contain harmonics up to 300 Hz for voltage and 600 Hz for current [8, 9].
- Asymmetry of the current waveform: a difference in the peak value and the shape of positive and negative half cycles in HIF current is present due to the difference between the breakdown voltage and the positive and negative voltage values [10, 11].

Main Points

- This study proposes a new algorithm aimed at both detecting high impedance faults (HIF) that often go undetected by conventional protection devices and discriminating the faulty phase.
- The algorithm leverages discrete wavelet transform (DWT) with the “sym5” mother wavelet and a 5-level multi-resolution analysis (MRA) that can effectively capture transient events such as HIF.
- The performance of the proposed algorithm was evaluated through simulation of 5 test cases on a simple medium voltage distribution system using MATLAB/Simulink 2022b.
- Performance of the proposed algorithm is compared with other algorithms discussed in the literature, accompanied by an examination of the limitations of the proposed method.

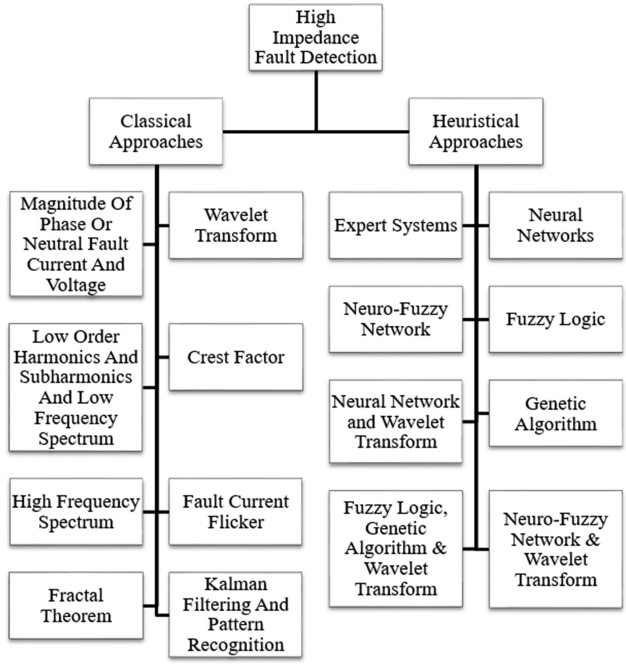

Fig. 1. Classification of high impedance fault detection approaches [12].

C. High Impedance Fault Detection Approaches

Various approaches were implemented and discussed in literature over the past years. Some of them are considered classical approaches that depend on classically extracting HIF features, and others are considered heuristic, which are based on intelligently decisive tools. Fig. 1 shows a classification table of HIF detection approaches [12].

1) Classical Approaches

Earlier approaches that are based on monitoring the magnitude of phase or neutral fault current and voltage like the ratio grounded relaying (RGR) algorithm [13], modified directional earth fault relay [14], and others were not precise and most of the time misinterpreted the conditions. Other approaches based on low order harmonics, sub-harmonics, low-frequency spectrum, and high frequency spectrum such as analyzing the spectral behavior of low frequency in terms of magnitude and phase [15], and the increase in energy level of harmonics and the degree of randomness associated with arcing HIFs [16] are considered good in terms of detection of HIF. This is due to the fact that such faults induce high- and low-frequency components to the system, resulting in harmonics and subharmonics being present in the current and voltage waveforms. Feature extractors such as wavelet transform can be considered one of the most used techniques for HIF detection due to

the fact that it can extract disturbances found in a signal and analyze them.

2) Heuristic Approaches

Heuristic approaches are mainly based on artificial intelligence (AI) and ML, such as fuzzy logic, neural networks, and genetic algorithms. Such approaches are trained to recognize patterns associated with HIF based on historical data. These methods need extensive training datasets, which is expensive. Furthermore, studies employing these methods are very few and still limited.

II. HIF DETECTION USING DISCRETE WAVELET TRANSFORM

A. Wavelet Transform

A wavelet transform (WT) is a mathematical tool used to analyze signals and functions in both time and frequency domains. The basic idea of a WT is to decompose a signal into small and well-localized functions called wavelets. WT uses wavelets that are well-localized in time and frequency. This allows for a more flexible representation of signals with localized features or sudden changes.

Wavelet transform has two main types: continuous WT (CWT) and discrete WT (DWT). CWT is defined as a continuous wavelet function scaled and translated across the signal. It provides a continuous analysis of the signal's frequency content at different scales by representing the signal in terms of the scale and location parameters. On the other hand, DWT is often more computationally efficient in practical applications. It involves a discrete set of scales and translations. A signal is decomposed into approximation coefficients (representing the coarse details) and detail coefficients (representing the fine details) at different scales. This decomposition is performed iteratively to create a multiresolution analysis (MRA) of the signal. Various applications need the use of WT such as signal processing, image compression, data compression, and feature extraction. They are precisely suited for analyzing signals that are characterized as non-stationary or time-varying.

B. Discrete Wavelet Transform

Discrete wavelet transform decomposes a discrete signal $x[n]$ into approximation coefficients ($a_j[n]$) and detail coefficients ($d_j[n]$) at different scales (or levels j). At each level of decomposition, the signal is split into two components: the approximation, which represents the low-frequency content, and the detail, which captures the high-frequency content. Decomposition is achieved using a pair of low-pass filters ($h[n]$) and high-pass filters ($g[n]$). The signal is convolved with these filters to obtain the approximation ($a_{j+1}[n]$) and detail ($d_{j+1}[n]$) coefficients using the following equations:

$$a_{j+1}[n] = \sum_k h[k].a_j[2n-k] \quad (1)$$

$$d_{j+1}[n] = \sum_k g[k].a_j[2n-k] \quad (2)$$

After convolution, the signal is downsampled by a factor of 2 to reduce its length and prepare for the next level of decomposition. The decomposition process is repeated iteratively until the desired level of resolution is reached or until the signal cannot be further decomposed. The original signal can be reconstructed from the approximation and detail coefficients using a synthesis process, which involves upsampling and convolution with the corresponding synthesis filters. Approximation coefficients ($a_j[n]$) capture the low-frequency content, while the detail coefficients ($d_j[n]$) capture the high-frequency content. DWT provides a MRA of the signal, meaning that it represents the signal at different levels of detail and resolution. The ability of DWT to represent signals in a hierarchical and localized manner makes it useful for analyzing signals with both smooth and rapidly changing components. Fig. 2 shows the level-wise signal decomposition of the discrete WT.

C. High Impedance Fault Modeling

A precise simulation of HIFs is essential for the implementation of effective HIF detection techniques. High impedance fault model data

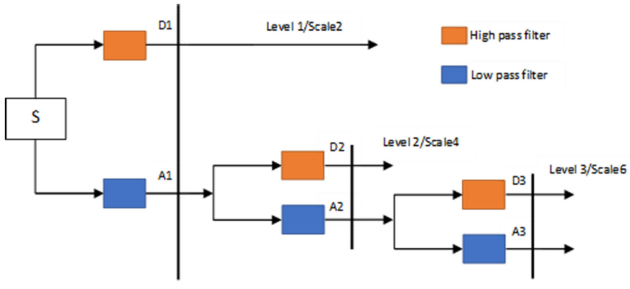

Fig. 2. Wavelet transform signal decomposition.

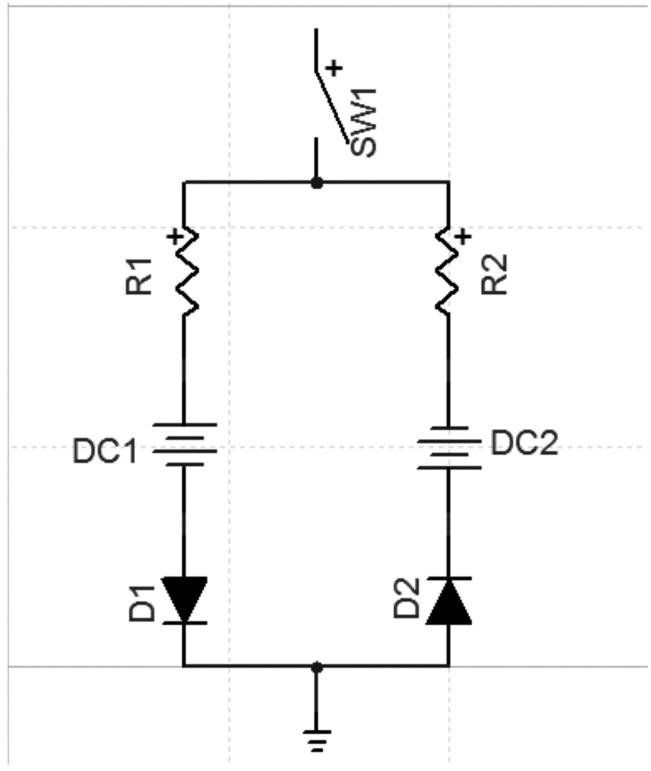

Fig. 3. T.M Lai [8] simplified Emanuel model [17].

TABLE I.
SIMPLIFIED EMANUEL MODEL R1 AND R2 PARAMETERS

R1	R2
205	210
212	222
236	227
255	271
270	286
283	289

should include a variety of characteristics of real-life HIFs such as asymmetry, randomness, nonlinearity, and dynamic qualities of arcing phenomena.

High impedance faults are usually accompanied with an arc; the model should include random and dynamic qualities of arcing. T. M. Lai's simplified HIF model combines most of the advantages of other models and maintains simplicity and accuracy.

The proposed model is based on T. M. Lai's simplified HIF model that is shown in Fig. 3. below, it includes two DC sources, DC1 and DC2, with voltages Vp and Vn, respectively, representing the arcing voltage of air in soil and/or between trees and the distribution line. There are also two resistances R1 and R2, placed between two diodes, D1 and D2, representing the resistance of trees and/or the earth resistance [17].

The simplified Emanuel model used in this study is based on arcing in sandy soil, and according to [18], HIF current in such cases is around 10A. According to other references such as [19], HIF current in dry soil is around 20A and for wet soil it is around 40A.

Variable resistances are used as R1 and R2, since the resistance in HIFs is not stable and it keeps on varying up and down, a sample resistance values R1 and R2 are represented in Table I. below. From the table, it can be seen that the average resistance is between 250 and 260 ohms. From this example, it can be concluded that the average variation in resistance for HIF is around 10%-15%.

Proposed HIF detection algorithm: the proposed algorithm to detect HIFs depends on discrete WT, which is known to be a great technique for analyzing signals in the time–frequency domain. Faults such as HIFs have significantly low current values and exhibit highly nonlinear characteristics, which leads to the presence of harmonics and high-frequency components. The WT is known for being a precise tool for extracting disturbances from a signal, which in this case is the high-frequency components. Discrete WT is modeled by using a multistage filter with the mother wavelet as the low-pass filter and it's dual as the high-pass filter. As a mother wavelet, the symlet wavelet was chosen, specifically the "sym5" is used. The reason for choosing symlet as a mother wavelet is that symlets are beneficial for preserving energy and aiding in signal analysis. Moreover, they can be effective in extracting important features from signals,

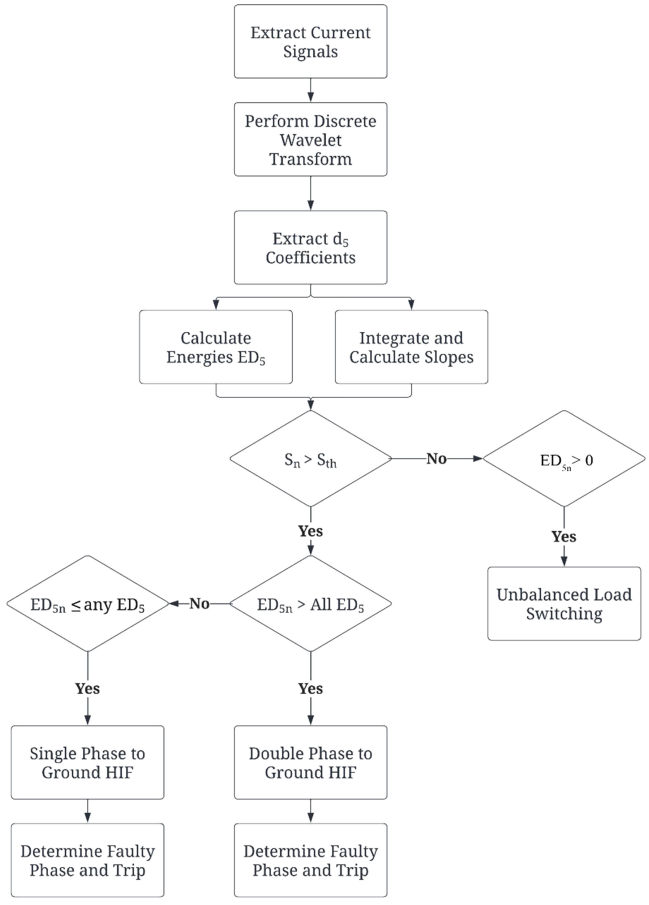

Fig. 4. Flowchart of proposed HIF detection algorithm.

making them valuable in applications such as pattern recognition and classification. Furthermore, they are considered versatile and can adapt to different signal characteristics, including signals with abrupt changes and discontinuities, which makes them suitable for analyzing signals that have features such as edges or spikes. A 5-level MRA decomposition is applied to analyze the current signals and extract their features.

1) HIF Detection Algorithm Flowchart
A flowchart of the proposed algorithm is shown in Fig. 4.

2) Algorithm Description
The proposed HIF detection algorithm is based on the analysis of the 5th level detail of the DWT performed on the current signals extracted from the transformer secondary winding. The algorithm can be summarized as follows:

- Extract current signals at transformer secondary for all phases and neutral.
- Perform DWT/MRA on current signals for all phases and the neutral using "sym5" as the mother wavelet and a 5-level decomposition.
- Extract and plot the detail d5 coefficients of the three-phase currents and neutral.
- Calculate the energy of detail d5 ED5 for all phases and neutral

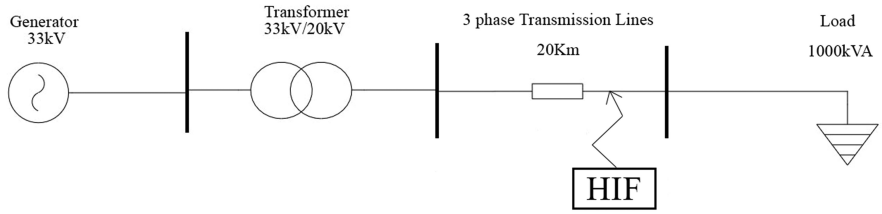

Fig. 5. Single line diagram of the model distribution system.

- Plot the area variation curve for the d5 coefficients and integrate and calculate the average slope of the slopes of all phases and the neutral.
- Threshold slope S_{th} is determined as 80 by doubling the maximum slope in the normal operating conditions, taking into consideration an unbalanced load switching.
- Compare the average neutral slope S_n and threshold slope and determine whether an HIF or unbalanced load switching is occurring.
- In the case of HIF, compare energies and determine if single or double phase to ground HIF.
- Trip faulty phase(s)

III. COMPUTER SIMULATION STUDIES FOR TESTING THE PROPOSED METHOD

A. Medium Voltage Distribution System Model For HIF Detection Studies

A single-line diagram of the test system that is used for HIF detection is shown in Fig. 5. A 33 kV three-phase source is connected to a two-winding 33/20 kV transformer that is connected to a three-phase transmission line which is in turn connected to a static load of power 800 kW at a rated power factor of 0.8 resulting in 1000 kVA. The system is grounded with low-resistance grounding to control the ground fault and limit the ground fault current in order to prevent damage to equipment in case of a ground fault by tripping the protective devices. The purpose of low-resistance grounding is to immediately cut the power to the circuit in case of a fault; it also reduces overvoltage.

Generator is grounded over an 80 Ω resistance and connected to the transformer which is Y-grounded/Y-grounded. The transformer is also grounded with a 50 Ω resistance in order to limit the fault current to 400A maximum in case of a ground fault. In grounded neutral systems, unbalanced currents and fault currents return back to the source through neutral return.

An HIF model is connected to phase C at the secondary of the transformer and simulated to extract the current waveform shown in Fig. 6. It is a typical HIF waveform which proves that this model simulates an HIF correctly. The random variation of resistance of HIFs introduces asymmetry to the fault current, and due to arc interruption at natural current zero, shoulders are present at zero crossings.

B. Computer Simulation Studies for the Performance Analysis of the Proposed Algorithm

1) Case 1: Normal Operation

Three-phase voltage and current waveforms at transformers secondary under normal operating conditions are shown in Fig. 7. There is no disturbance on the voltage and current signals as it is expected.

Three-phase and neutral current signals are analyzed using DWT/MRA with “sym5” as the mother wavelet. D5 coefficients of all

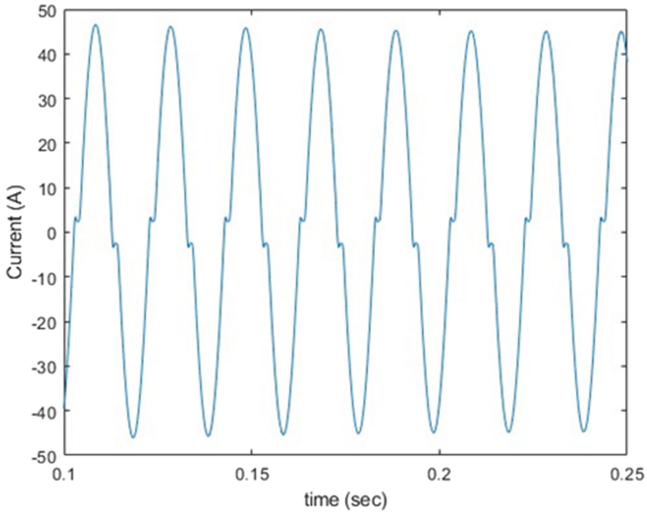

Fig. 6. HIF Current waveform.

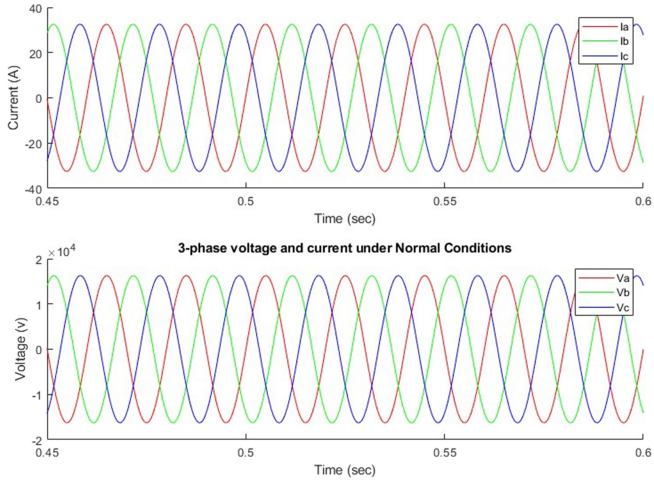

Fig. 7. Three-phase voltage and current at the transformer secondary under normal operating conditions.

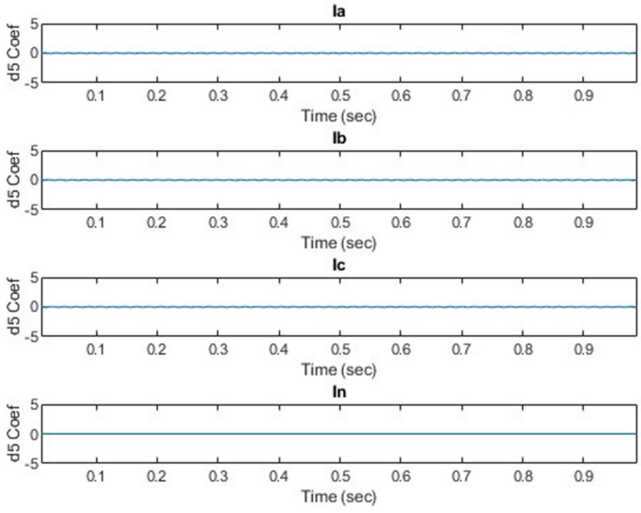

Fig. 8. D5 coefficients of all phases and the neutral under normal operating conditions.

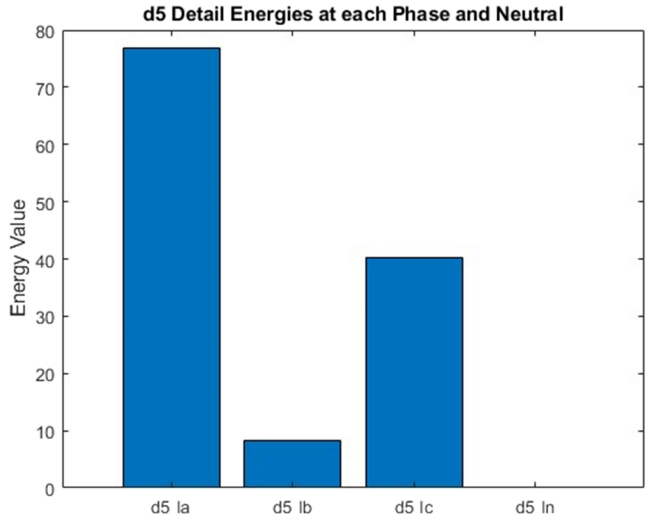

Fig. 10. Energy of d5 for all phases and neutral under normal operating conditions.

phases and neutral at the secondary of the transformer are plotted in Fig. 8. It is clear that no high frequency components are present under normal operating conditions.

To develop a fault index, the absolute values of the d5 coefficients are calculated and summed up to form area variation curve, which is then integrated with respect to time to form the slope variation curve shown in Fig. 9. Since the system is in normal operating conditions, neither a change in area nor in slope is detected, and average slope values are so small, around 40.

Energy of level d5 is calculated and plotted in Fig. 10. Energies are relatively small and no energy is present in the neutral at all.

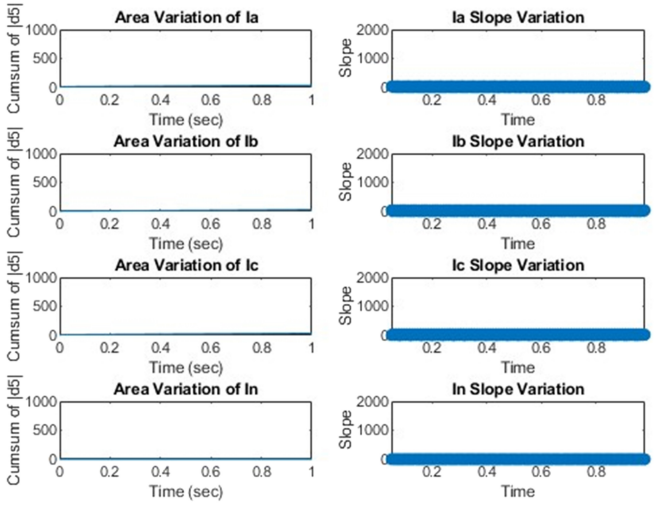

Fig. 9. Area variation (left) and slope variation (right) curves under normal operating conditions.

2) Case 2: HIF at the End of the Transmission Line Related to Phase A

Three-phase voltage and current waveforms at the transformer's secondary terminal under a single-phase HIF related to phase A are shown in Fig. 11. It is clear that at the instant of the fault, current increased as if there were a change in the load, but no changes in the voltage waveform was recorded.

Three-phase and neutral current signals are analyzed using DWT/MRA with "sym5" as the mother wavelet. D5 coefficients of all phases and neutral at the secondary of the transformer are plotted in Fig. 12. At the instant of HIF at 0.5 sec, disturbances in d5 coefficients start appearing in phase A and the neutral due to high-frequency components from the HIF.

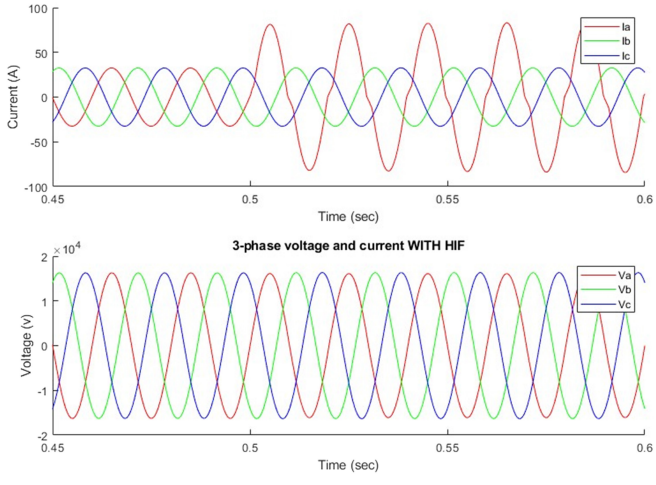

Fig. 11. Three-phase voltage and current at the transformer secondary under the HIF case on phase A.

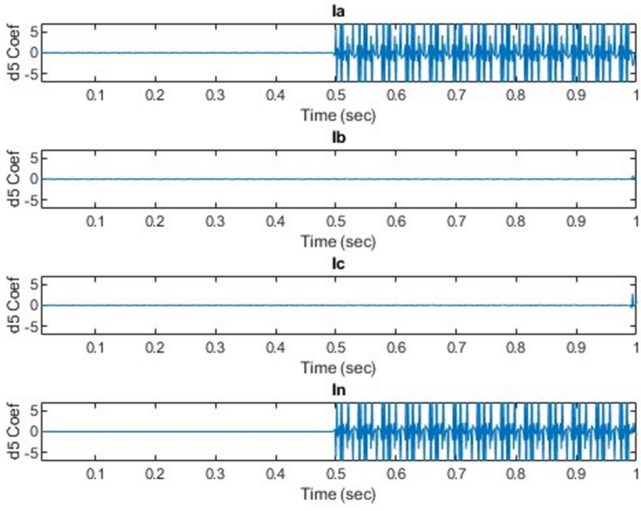

Fig. 12. D5 coefficients of all phases and neutral with HIF at phase A.

The absolute values of the d5 coefficients are calculated and summed up to form area variation curve, which is then integrated with respect to time to form the slope variation curve shown in Fig. 13. The area under the curve will increase for any disturbance in the d5 coefficients, but for a permanent disturbance at 0.5 seconds due to HIF, the area keeps on increasing as long as the fault lasts. In this situation, the areas of phase A and the neutral started increasing at 0.5 seconds and kept increasing since the fault is still present. As a result, slopes of phase A and the neutral changes and increased and average slopes whooped a huge increase, and S_n increased up to around 3400.

Energy of level d5 is calculated and plotted in Fig. 14. Energies at faulty phase A and the neutral are relatively equal and very high with respect to energies of the two other phases.

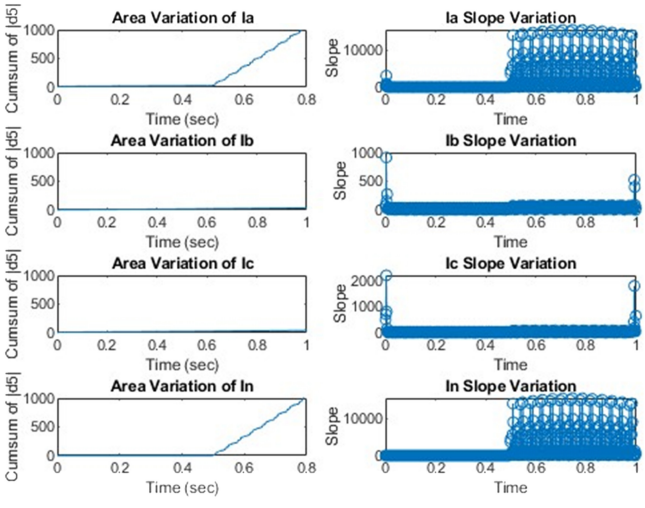

Fig. 13. Area variation (left) and slope variation (right) curves with HIF at phase A.

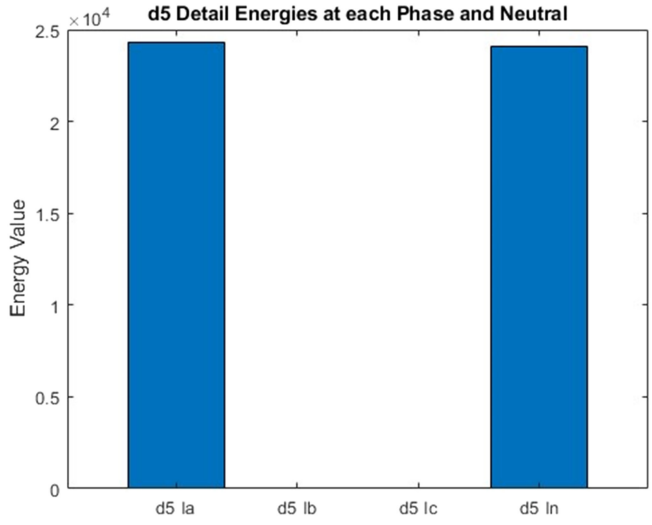

Fig. 14. Energy of d5 for all phases and neutral with HIF at phase A.

3) Case 3: HIF at the End of the Transmission Line Related to Phases A and B

Three-phase and neutral current signals are analyzed using DWT/MRA with "sym5" as the mother wavelet. D5 coefficients of all phases and neutral at the secondary of the transformer are plotted in Fig. 15, at the instant of HIF at 0.5 sec, disturbances in d5 coefficients start appearing in phases A and B, along with the neutral, due to high frequency components from the HIF.

The absolute values of the d5 coefficients are calculated and summed up to form area variation curve, which is then integrated with respect to time to form the slope variation curve shown in Fig. 16. The area under the curve will increase for any disturbance in the d5 coefficients, but for a permanent disturbance at 0.5 seconds due to HIF, the area keeps on increasing as long as the fault lasts. In this situation, the areas

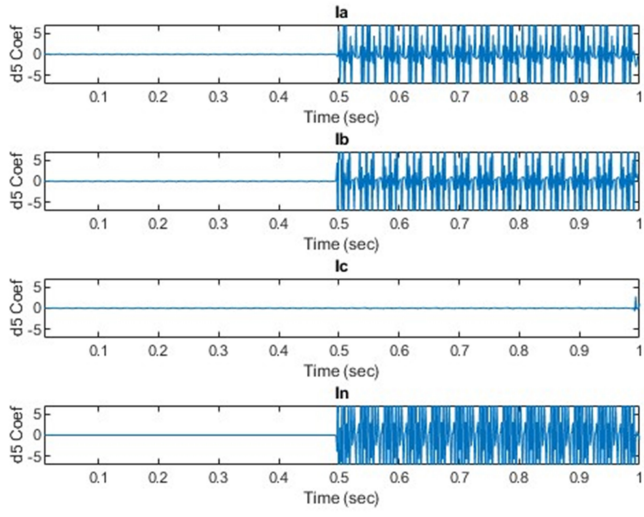

Fig. 15. D5 coefficients of all phases and neutral with HIF at phases A and B.

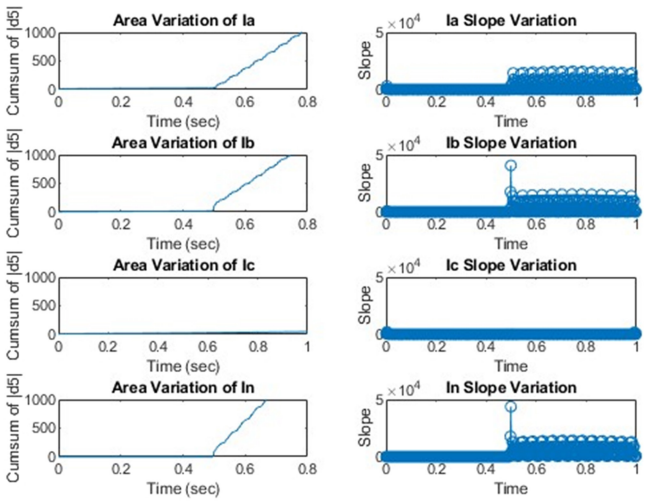

Fig. 16. Area variation (left) and slope variation (right) curves with HIF at phases A and B.

of phases A and B and the neutral started increasing at 0.5 seconds and kept increasing since the fault is still present. As a result, slopes of phases A and B and the neutral changes and increased and average slopes whooped a huge increase, and S_n increased to around 5600 as shown in Fig. 16.

Energy of level d5 is calculated and plotted in Fig. 17. Energies at faulty phases A and B and the neutral are very high with respect to energies of the other phases. Also, energy in the neutral is the highest.

C. Limitations in the Performance of the Algorithm

After conducting several tests and simulations, some limitations to the proposed method were detected.

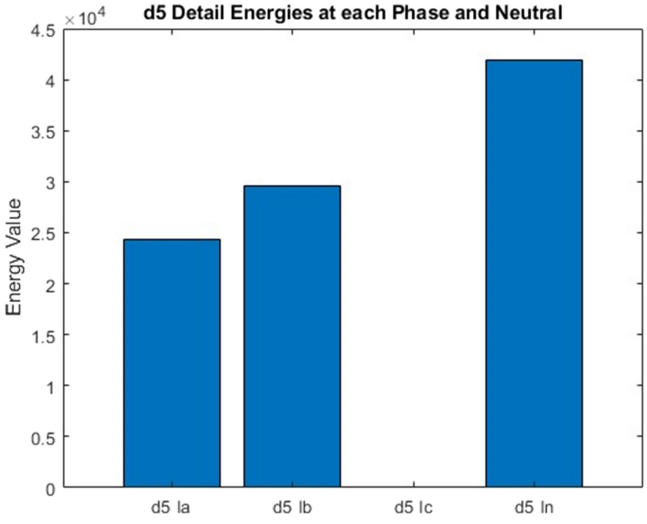

Fig. 17. Energy of d5 for all phases and neutral with HIF at phases A and B.

TABLE II.
VOLTAGE AND RESİSTANCE VALUES OF THE HIGH IMPEDANCE FAULT MODEL

R1	R2	DC1	DC2
6000 Ω	6100 Ω	3862 V	3268 V

For higher fault current (lower impedance levels), the algorithm worked perfectly without any limitations. However, for lower fault current (higher impedance levels), some issues started appearing. Everything works totally fine, and the algorithm gives great results for fault currents above or equal to 10 A, which means resistances below 2000 Ω. For currents between 5.5A and 10A (2000 Ω < R < 5000 Ω) the algorithm still works but on a risky margin because very low high-frequency components are present in the d5 coefficients. While current levels below 5.5 A (R >5500 Ω) are successful in terms of HIF detection, but high-frequency components are very low in the d5 coefficients (around 0), resulting in relatively low average slope levels in the neutral and in addition to very similar energy of details levels in all phases and neutral, resulting in a failure in detecting the faulty phase.

It is to be noted that for high levels of fault currents that may be above tripping levels of overcurrent relays or other protection devices, the algorithm is not needed since automatic tripping will happen. And for very high-resistance values which are considered infinite, the fault current will be relatively equal to zero so no fault appears.

An example of the limitation is illustrated below, HIF is injected to phase B, and voltages and resistances of the model are shown in Table II.

The algorithm responses are shown in Figs. 18, 19, and 20.

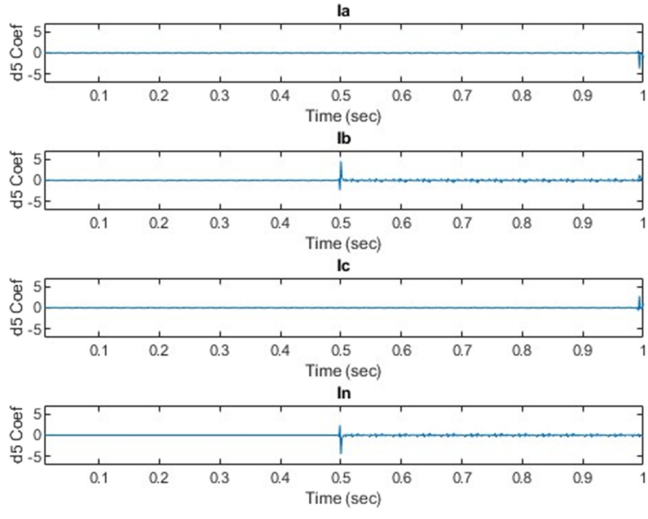

Fig. 18. D5 coefficients of all phases and neutral with HIF at phase B (limitation).

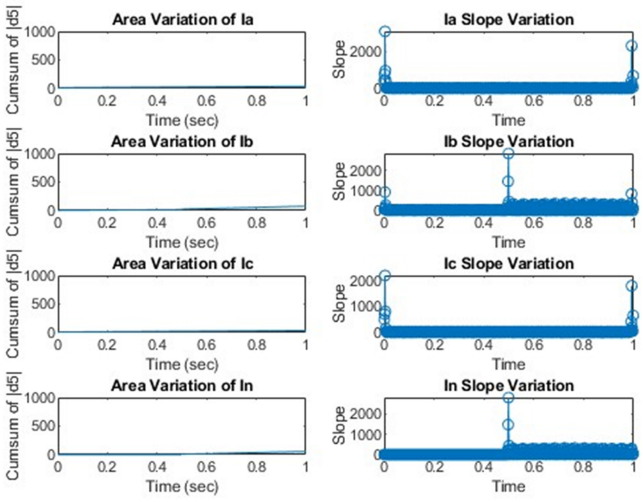

Fig. 19. Area variation (left) and slope variation (right) curves with HIF at phase B (limitation).

Areas of phase B and the neutral slightly increased after HIF instance at 0.5 sec. As a result, slopes of phase B and the neutral slightly increased and average slopes showed a very low increase. Sn increased to around 95.65.

Energy levels at each phase and neutral are shown in Fig. 20. It is clear that energy levels are relatively low and energy of the faulty phase is not the largest.

Fault current in this case was around 4.8A. The high frequency components are very low. From that, the area variation curve shows a very slight increase with time, resulting in average slope levels that are relatively low. The faulty phase energy level (phase B) is lower

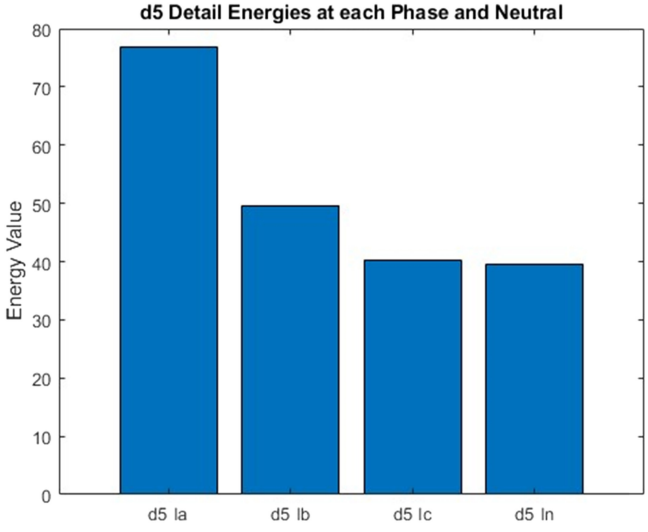

Fig. 20. Energy of d5 for all phases and neutral with HIF at phase B (limitation).

than that of phase A, which gives a false interpretation of the algorithm and causes the wrong phase to be tripped.

4) Discussion on Comparative Performance

Traditional protection devices, such as overcurrent protection and distance protection, face challenges in detecting HIF due to their reliance on current level measurements and system impedance analysis. Overcurrent protection is insufficient for HIF detection as these faults generate low currents below predefined thresholds. Distance protection struggles with HIFs' high impedance values, leading to overreach or underreach in fault detection. Fourier transform, commonly used for HIF detection, lacks precise time and frequency resolution, especially for intermittent and non-stationary HIFs. The smearing effect in Fourier makes it challenging to distinguish frequency components accurately. AI and ML methods, such as genetic algorithms and neural networks, show promise for HIF detection, but they require extensive training datasets which may be expensive. Moreover, studies on these methods are limited.

In studies leveraging WT analysis to detect HIF, most authors concentrate on the detection of HIF rather than discrimination. However, this study places emphasis on both detection and discrimination of HIF, leading to improved precision and overall algorithm performance. Limitation comparisons with other algorithms are not feasible due to insufficient information about the limitations of those alternative methods.

IV. CONCLUSION

This study sheds light on a very important and vital issue that may be the most controversial problem in distribution systems, which is the HIF. That is because of the difficulties and challenges in the process of detecting such faults, due to the randomness and relatively low fault current they produce. In this study, a new HIF detection algorithm is proposed, which is based on discrete WT. In the proposed algorithm, discrete WT with "sym5" mother wavelet and a five-level MRA is done, and then the energies of the fifth detail at each phase and the neutral are calculated. Also, the area variation graph was extracted along with a slope variation graph, and after that, average slopes were calculated and compared to a threshold value to detect if there was a fault or other conditions. Average slope values along with energies of details (ED5) are used to come up with an algorithm for detecting HIFs. Testing of the proposed method is performed by simulation using MATLAB and Simulink 2022b software.

The simulation results indicate that a potentially precise HIF detection algorithm was proposed. The proposed algorithm was successful in differentiating between an unbalanced load switching condition and an HIF situation. Moreover, the proposed method proved to be precise in detecting if a single-phase HIF or double-phase HIF is occurring from different energy values, in addition to detecting the faulty phase or phases present in the system.

The development and implementation of the HIF detection algorithm proposed in this study are still at their first stages. Due to the fact that an HIF is very difficult to model in a perfect way, computer simulation results carried out by MATLAB and Simulink may not be

that precise and may be different than real-life situations. Real-life testing and analysis must be performed to verify the precision of the proposed algorithm. Moreover, the simulation was done on a simple distribution system, so the algorithm should also be tested on more complicated systems, and more sophisticated cases should be considered. Last, future work to find the fault location can be done to increase the reliability of this algorithm.

Peer-review: Externally peer-reviewed.

Author Contributions: Concept – B.M., O.U.; Design – B.M.; Supervision – O.U.; Resources – B.M.; Materials – B.M.; Data Collection and/or Processing – B.M.; Analysis and/or Interpretation – B.M.; Literature Search – B.M.; Writing – B.M., O.U.; Critical Review – B.M., O.U.

Declaration of Interests: The authors have no conflicts of interest to declare.

Funding: This study received no funding.

REFERENCES

1. C. J. Kim, B. D. Russell, and K. Watson, "A parameter-based process for selecting high impedance fault detection techniques using decision making under incomplete knowledge," in *IEEE Trans. Power Deliv.*, vol. 5, no. 3, pp. 1314–1320, 1990. [CrossRef]
2. A.-R. Sedighi, M.-R. Haghifam, O. P. Malik, and M.-H. Ghassemian, "High impedance fault detection based on wavelet transform and statistical pattern recognition," in *IEEE Trans. Power Deliv.*, vol. 20, no. 4, pp. 2414–2421, 2005. [CrossRef]
3. J. R. Macedo, J. W. Resende, C. A. Bissochi, D. Carvalho, and F. C. Castro, "Proposition of an interharmonic-based methodology for high-impedance fault detection in distribution systems," *IET Gener. Transm. Distrib.*, vol. 9, no. 16, pp. 2593–2601, 2015. [CrossRef]
4. A. Hamel, A. Gaudreau, and M. Cote, "Intermittent arcing fault on underground low-voltage cables," in *IEEE Trans. Power Deliv.*, vol. 19, no. 4, pp. 1862–1868, 2004. [CrossRef]
5. M. Carpenter, R. R. Hoad, T. D. Bruton, R. Das, S. A. Kunsman, and J. M. Peterson, "Staged-fault testing for high impedance fault data collection," 58th Annual Conference for Protective Relay Engineers, College Station, TX, USA, 2005, pp. 9–17. [CrossRef]
6. E. Acha, A. Semlyen, and N. Rajakovic, "A harmonic domain computational package for nonlinear problems and its application to electric arcs," in *IEEE Trans. Power Deliv.*, vol. 5, no. 3, pp. 1390–1397, 1990. [CrossRef]
7. L. U. Iurinic, A. D. Filomena, A. S. Bretas, and R. G. Ferraz. IET Conference Publications, pp. 6.2.3–6.2.3, 2014. [CrossRef]
8. T. M. Lai, L. A. Snider, E. Lo, and D. Sutanto, "High-impedance fault detection using discrete wavelet transform and frequency range and RMS conversion," in *IEEE Trans. Power Deliv.*, vol. 20, no. 1, pp. 397–407, 2005. [CrossRef]
9. T. M. Lai, L. A. Snider, and E. Lo, "Wavelet transform based relay algorithm for the detection of stochastic high impedance faults," *Electr. Power Syst. Res.*, vol. 76, no. 8, pp. 626–633, 2006. [CrossRef]
10. A. F. Sultan, G. W. Swift, and D. J. Fedirchuk, "Detecting arcing downed-wires using fault current flicker and half-cycle asymmetry," in *IEEE Trans. Power Deliv.*, vol. 9, no. 1, pp. 461–470, 1994. [CrossRef]
11. N. Zamanan, and J. K. Sykulski, "Modelling arcing high impedances faults in relation to the physical processes in the electric arc," *WSEAS Trans. Power Syst.*, vol. 1, pp. 507–512, 2006.
12. M. Sedighizadeh, A. Rezazadeh, and N. I. Elkalashy, "Approaches in high impedance fault detection - A chronological review," *Adv. Electr. Comput. Eng.*, vol. 10, no. 3, pp. 114–128, 2010. [CrossRef]
13. R. E.Lee, and M. T.Bishop, "Performance testing of the ratio ground relay on a four-wire distribution feeder," *IEEE Trans. Power Apparatus Syst.*, vol. 9, pp. 2943–2949, 1983. [CrossRef]
14. Z. Gan, X. Z. Dong, Z. Q. Bo, B. R. J. Caunce, and D. Montjean, "A new protection scheme for high impedance fault using adaptive trip and recloser technique," *Proceedings International Conference on Power System Technology*, vol. 1, pp. 295–299, 2002.
15. A. G. Phadke, and H. E. Hankun, "Detection of broken distribution conductors," in *Proceedings IEEE Southern Conference, Raleigh, N. C.*, CH2161–2168/85/0000-0074.
16. C. L. Benner, P. W. Carswell, and B. D. Russell, "Improved algorithm for detecting arcing faults using random fault behavior," *Electric Power Systems Research Southern Electric Industry Application Symposium, New Orleans*, vol. 17, no. 1, pp. 49–56, 1989. [CrossRef]
17. G. N. Lopes, V. A. Lacerda, J. C. M. Vieira, and D. V. Coury, "Analysis of signal processing techniques for high impedance fault detection in distribution systems," in *IEEE Trans. Power Deliv.*, vol. 36, no. 6, pp. 3438–3447, 2021. [CrossRef]
18. D. Kumar, A. Kumar, R. Singh, and M. Sarwar, "Detection of high impedance fault in low voltage distribution system using discrete wavelet transform," 2nd International Conference for Innovation in Technology (INOCON), Bangalore, India, vol. 2023, 2023, pp. 1–5. [CrossRef]
19. A. H. Eldin, N. Mohamed, and E. Abdallah. IET Conference Publications, vols. 1–4, pp. 0202–0202, 2013. [CrossRef]